Supplementary Information for
"Linkage disequilibrium dependent architecture of human complex traits shows action of negative selection"

Supplementary Note

Proof of the extension of stratified LD score regression to continuous annotations.
The derivation of stratified LD score regression using binary annotations has previously been described[1]. Here, we extend the method to continuous-valued annotations.

Suppose that we have a sample of N individuals, and a vector $y = (y_1, \dots, y_N)$ of quantitative phenotypes, standardized to mean 0 and variance 1. We assume the infinitesimal linear model

$$y = X\beta + \varepsilon \tag{1}$$

where X is a N x M matrix of standardized genotypes, $\beta = (\beta_1, \dots, \beta_M)$ is the vector of per normalized genotype effect size, and $\varepsilon = (\varepsilon_1, \dots, \varepsilon_N)$ is a mean-0 vector of residuals with variance σ_e^2. Here, we are interested in modeling β as a mean-0 vector whose variance depends on C continuous-valued annotations $a_1, \dots, a_C$:

$$Var(\beta_j) = \sum_c a_c(j)\tau_c \tag{2}$$

where $a_c(j)$ is the value of annotation a_c at SNP j, and τ_c represents the per-SNP contribution of one unit of the annotation a_c to heritability. This is a generalization of stratified LD score regression[1], with $a_c(j) \in \{0,1\}$ if annotation a_c has binary values.

Let $\hat{\beta}_j$ be the estimate of the marginal effect of SNP j in our sample. According to Finucane et al.[1], we can write

$$\hat{\beta}_j = \sum_k \hat{r}_{jk}\beta_k + \varepsilon_j' \tag{3}$$

where $\hat{r}_{jk} := \frac{1}{N} X_j^t X_k$ is the in-sample correlation between SNPs j and k, and $\varepsilon_j' = X_j^t \varepsilon / N$ (ε_j' has mean 0 and variance σ_e^2/N).

We define $\chi_j^2 := N\hat{\beta}_j^2$ (as in ref. [1]). We can write

$$
\begin{aligned}
E\left[\chi_j^2\right] &= NE\left[\hat{\beta}_j^2\right] \\
&= NE\left[\left(\sum_k \hat{r}_{jk}\beta_k + \varepsilon_j'\right)^2\right] \\
&= N\sum_k E\left[\hat{r}_{jk}^2\right]E\left[\beta_k^2\right] + NE\left[\left(\varepsilon_j'\right)^2\right] \\
&= N\sum_k \left(E\left[\hat{r}_{jk}^2\right]\sum_c a_c(k)\tau_c\right) + N(\sigma_e^2/N) \\
&= N\sum_c \left(\tau_c \sum_k a_c(k)E\left[\hat{r}_{jk}^2\right]\right) + \sigma_e^2
\end{aligned}
\tag{4}
$$

where the third equality holds because $\hat{r}_{jk}$, β_k, and ε_j' are independent and β and ε' have mean 0. Note that r_{jk} denotes the true correlation between SNPs j and k in the underlying population and that r_{jk} is fixed throughout, so that $\hat{r}_{jk}$ and β_k are independent even though both depend on r_{jk}. In an unstructured sample, we have $E\left[\hat{r}_{jk}^2\right] \approx r_{jk}^2 + 1/N$. We thus have

$$
\begin{aligned}
E\left[\chi_j^2\right] &\approx N\sum_c \left(\tau_c \sum_k a_c(k)\left(r_{jk}^2 + 1/N\right)\right) + \sigma_e^2 \\
&= N\sum_c \left(\tau_c \sum_k a_c(k) r_{jk}^2\right) + N\sum_c \left(\tau_c \sum_k a_c(k)/N\right) + \sigma_e^2 \\
&= N\sum_c \left(\tau_c \sum_k a_c(k) r_{jk}^2\right) + \sum_k \sum_c (a_c(k)\tau_c) + \sigma_e^2 \\
&= N\sum_c \tau_c l(j,c) + \sum_k Var(\beta_k) + \sigma_e^2
\end{aligned}
\tag{5}
$$

where $l(j,c) = \sum_k a_c(k) r_{jk}^2$ is the LD score of SNP j with respect to annotations a_c. As the variance of our phenotype y is $\sum_k Var(\beta_k) + \sigma_e^2$ and is equal to 1 by definition, this reproduces the main equation of stratified LD score regression (modulo the term *Nb* for confounding biases):

$$
E\left[\chi_j^2\right] = N\sum_c \tau_c l(j,c) + 1 \tag{6}
$$

Application of stratified LD score regression

Reference SNPs, used to estimate LD scores, were defined as the set of 9,997,231 biallelic SNPs with minor allele count greater or equal than five in the set of 489 unrelated and outbred European samples[2] from phase 3 of 1000 Genomes Project (1000G)[3] (see URLs). Regression SNPs, used to estimate the vector of τ from GWAS summary statistics, were defined as the set of 1,217,312 HapMap Project Phase 3 SNPs, used here as a proxy for well-imputed SNPs. SNPs with unusual χ^2 association statistics (larger than 80 or $0.0001N$), as well as SNPs in the major histocompatibility complex (MHC) region (chr6:25Mb-34Mb) were removed from all analyses. We note that the choice of regression SNPs is distinct from the choice of reference SNPs, and that regression SNPs tag potentially causal reference SNPs via LD scores computed using reference SNPs (see ref. [1] for further details). Heritability SNPs, used to compute sd_c, h_g^2 and $h_g^2(C_{c,q})$, were the set of 5,961,159 reference SNPs with MAF $\geq$ 0.05. To assess the reproducibility of our results, we also considered 3,567 individuals of UK10K database[4] (ALSPAC and TWINSUK cohorts) as a reference panel. We had 13,326,465 reference SNPs and 5,353,593 heritability SNPs in this analysis.

Coalescent simulations to assess the link between LLD and allele age.

Coalescent simulations were performed using ARGON software[5] (see URLs) to assess the correlation between the LLD and MAF-adjusted allele age of a SNP. We used demographical model parameters estimated in Gravel et al.[6] to simulate European and African human genetic data, and assumed a generation time of 25 years. Recombination rate was set to 1 cM/Mb and mutation rate to 1.65 x 10^{-8} (ref. [7]). We generated 33 fragments of 100 Mb for 500 European and 500 African individuals, representing a realistic genome size and sample sizes equivalent to the reference populations of 1000G. LD scores were computed independently in each 100 Mb fragment on SNPs with an allele count $\geq$ 5 in Europeans, and allele age and LD scores were MAF-adjusted via MAF-stratified quantile normalization after merging the 33 fragments.

Psychiatric and autoimmune diseases analyses.

For analyses of psychiatric and autoimmune diseases, we considered five psychiatric diseases with low sample overlap (anorexia, autism, bipolar disorder, depressive symptoms and schizophrenia) and six autoimmune diseases with low sample overlap (celiac, cirrhosis, eczema, lupus, inflammatory bowel disease and rheumatoid arthritis). We meta-analyzed standardized effect sizes τ^* for the five psychiatric diseases and six autoimmune diseases using random effects, and compared the results with results for non-psychiatric and non-autoimmune diseases using a *z*-test. Non-psychiatric and non-autoimmune diseases were defined by removing psychiatric diseases and autoimmune diseases from the set of 31 independent traits, leading to a total of 28 and 29 traits, respectively.

23andMe data set.

For the 23andMe study, participants were drawn from the customer base of 23andMe Inc. (Mountain View, CA), a consumer genetics company[8,9]. All participants included in the analyses provided informed consent and answered surveys online according to the 23andMe human subjects protocol, which was reviewed and approved by Ethical & Independent Review Services, a private institutional review board. Samples were genotyped on one of four genotyping platforms. The V1 and V2 platforms were variants of the Illumina HumanHap550+ BeadChip, including about 25,000 custom SNPs selected by 23andMe, with a total of about 560,000 SNPs. The V3 platform was based on the Illumina OmniExpress+ BeadChip, with custom content to improve the overlap with our V2 array, with a total of about 950,000 SNPs. The V4 platform in current use is a fully custom array, including a lower redundancy subset of V2 and V3 SNPs with additional coverage of lower-frequency coding variation, and about 570,000 SNPs.

Participants were restricted to a set of individuals who have > 97% European ancestry, as determined through an analysis of local ancestry[10]. A maximal set of unrelated individuals was chosen for each analysis using a segmental identity-by-descent (IBD) estimation algorithm[11]. Individuals were defined as related if they shared more than 700 cM IBD, including regions where the two individuals share either one or both genomic segments identical-by-descent. This level of relatedness (roughly 20% of the

genome) corresponds approximately to the minimal expected sharing between first cousins in an outbred population.

Participant genotype data were imputed against the March 2012 "v3" release of 1000 Genomes reference haplotypes, phased with ShapeIt2 (ref. [12]). Data were phased and imputed for each genotyping platform separately. Data were phased using a 23andMe developed phasing tool, Finch, which implements the Beagle haplotype graph-based phasing algorithm[13], modified to separate the haplotype graph construction and phasing steps.

In preparation for imputation, phased chromosomes were split into segments of no more than 10,000 genotyped SNPs, with overlaps of 200 SNPs. SNPs with Hardy-Weinberg equilibrium $P < 10^{-20}$, call rate < 95%, or with large allele frequency discrepancies compared to European 1000 Genomes reference data were excluded. Frequency discrepancies were identified by computing a 2x2 table of allele counts for European 1000 Genomes samples and 2000 randomly sampled 23andMe participants with European ancestry, and identifying SNPs with a chi squared $P < 10^{-15}$. Each phased segment was imputed against all-ethnicity 1000 Genomes haplotypes (excluding monomorphic and singleton sites) using Minimac2 (ref. [14]), using 5 rounds and 200 states for parameter estimation.

The genetic association tests were performed using either linear or logistic regression as required assuming an additive model for allelic effects and controlled for age, sex, and five principal components of genetic ancestry.

UK Biobank data set.

We analyzed data from the UK Biobank (see URLs) consisting of 152,249 samples genotyped on ~800,000 SNPs and imputed to ~73 million SNPs. One individual who had withdrawn consent was removed, leaving 152,248 samples (see URLs, Genotyping and QC). We selected 15 phenotypes with large sample size. For each phenotype, we computed mixed model association statistics on up to 145,416 European-ancestry samples using version 2.2 of BOLT-LMM software[15] (see URLs) with genotyping array (UK BiLEVE / UK Biobank) and assessment center as covariates. We included 607,518 directly genotyped SNPs in the mixed model (specifically, all autosomal biallelic SNPs

with missingness < 2 % and consistent allele frequencies between the UK BiLEVE array and the UK Biobank arrays), and we computed association statistics on imputed SNPs in HapMap3 (1,186,683 SNPs on average over the 15 phenotypes). Heritability enrichment analyses of UK Biobank data were based on analyses of summary statistics, despite the availability of individual-level data, both to ensure consistency with the remaining 48 summary statistic data sets and because we are not currently aware of a heritability enrichment method applicable to individual-level data that can analyze a large number of overlapping or continuous-valued annotations.

Supplementary Tables

See Supplementary Excel file

Supplementary Table 1: Summary statistics data sets analyzed. We report the reference, sample size *N*, heritability *z*-scores and URLs (for publicly available summary statistics) for the 62 data sets analyzed in the manuscript. We also report the traits used in our meta-analysis, and in the psychiatric diseases / autoimmune diseases analyses. We note that for some traits there exist larger data sets using custom arrays with content targeted at known loci for specific diseases or traits (e.g. Immunochip, Metatabochip, etc.). We did not include those data sets, as stratified LD score regression is not applicable to data from those arrays[1].

See Supplementary Excel file

Supplementary Table 2: Effect size and statistical significance of the 13 LD-related annotations in each of 62 data sets analyzed. We report the standardized effect size (τ^*) and corresponding standard error and statistical significance of the 13 selected LD-related annotations conditioned on 10 MAF bins. Results of age at menarche and BMI are meta-analyzed over the different datasets (via fixed-effects meta-analysis) as we did not observe any sample overlap.

See Supplementary Excel file

Supplementary Table 3: Effect size and statistical significance of each LD-related annotation, meta-analyzed over 31 independent traits. We report the meta-analyzed standardized effect size (τ^*) and corresponding standard error and statistical significance of the 43 LD-related annotations conditioned on 10 MAF bins (two first columns) and conditioned on the baseline model and 10 MAF bins (two last columns).

See Supplementary Excel file

Supplementary Table 4: Correlation between all LD-related annotations and main functional annotations of the baseline model. We report correlations computed on common SNPs (MAF $\geq$ 5%).

	τ^* (se)	*P* value
LLD	-0.18 (0.04)	1.25E-06
LLD-D'	0.00 (0.03)	0.95
LLD-REG	0.03 (0.03)	0.37
Predicted Allele Age	-0.15 (0.03)	2.09E-06
LLD-AFR	-0.32 (0.03)	1.15E-24
Recombination Rate (10 kb)	-0.26 (0.02)	1.97E-33
Nucleotide Diversity (10 kb)	-0.29 (0.02)	4.76E-40
Background Selection Statistic	0.19 (0.02)	4.52E-24
GC-Content (1,000 kb)	0.00 (0.02)	0.99
CpG-Content (50 kb)	0.09 (0.02)	2.57E-07
Replication Timing	0.01 (0.04)	0.70
Centromeres (5 Mb)	-0.03 (0.01)	6.95E-07

Supplementary Table 5: Effect size and statistical significance of 12 LD-related annotations fitted jointly with 10 MAF bins. We report the meta-analyzed standardized effect size (τ^*) and corresponding standard error and statistical significance of 12 LD-related annotations fitted jointly with 10 MAF bins. These 12 annotations are significant when fitted independently and conditioned on 10 MAF bins. Results are meta-analyzed across 31 independent traits. LLD-D', LLD-REG, GC-content and replication timing are no longer significant when fitted jointly with a total of 12 LD-related annotations.

	τ^* (se)	*P* value
LLD	-0.16 (0.03)	1.10E-07
Predicted Allele Age	-0.17 (0.04)	1.05E-05
LLD-AFR	-0.30 (0.03)	3.30E-22
Recombination Rate (10 kb)	-0.27 (0.03)	2.98E-25
Nucleotide Diversity (10 kb)	-0.29 (0.02)	1.49E-30
Background Selection Statistic	0.19 (0.02)	3.85E-15
CpG-Content (50 kb)	0.06 (0.01)	2.64E-07
Centromeres (5 Mb)	-0.03 (0.01)	5.64E-07

Supplementary Table 6: Effect and statistical significance of eight LD-related annotations fitted jointly with 10 MAF bins. We report the meta-analyzed standardized effect size (τ^*) and corresponding standard error and statistical significance of eight LD-related annotations fitted jointly with 10 MAF bins. These 8 annotations remained significant when fitted jointly with a total of eight LD-related annotations and conditioned on 10 MAF bins. Results are meta-analyzed across 31 independent traits.

See Supplementary Excel file

Supplementary Table 7: Effect size and statistical significance of the 13 LD-related annotations conditioned on the baseline model in each of 62 data sets analyzed. We report the effect size (τ^*) and corresponding standard error and statistical significance of the 13 selected LD-related annotations conditioned on the baseline model and 10 MAF bins. Results of age at menarche and BMI are meta-analyzed over the different datasets (via fixed-effects meta-analysis) as we did not observe any sample overlap.

	τ^* (se)	*P* value
Predicted Allele Age	-0.24 (0.02)	1.08E-23
LLD-AFR	-0.20 (0.02)	4.20E-24
Recombination Rate (10 kb)	-0.20 (0.02)	2.55E-20
Nucleotide Diversity (10 kb)	-0.13 (0.02)	1.28E-11
Background Selection Statistic	0.11 (0.01)	4.90E-15
CpG-Content (50 kb)	0.23 (0.03)	2.53E-12

Supplementary Table 8a: Effect size and statistical significance of the six LD-related annotations of the baseline-LD model. We report the meta-analyzed effect size (τ^*) and corresponding standard error and statistical significance of the six LD-related annotations in the baseline model (i.e. fitted jointly with baseline model and 10 MAF bins). Results are meta-analyzed across 31 independent traits.

See Supplementary Excel file

Supplementary Table 8b: Heritability estimated using the baseline-LD model in each of 62 data sets analyzed. For each data set, we report the estimated heritability and corresponding standard error. We also furnished heritability estimates when using the original baseline model from Finucane et al.[1], and the baseline model used in this article (i.e. Finucane et al. baseline model + super/typical enhancer annotations + GERP annotations + 10 MAF bins).

See Supplementary Excel file

Supplementary Table 8c: Enrichment for all functional binary annotations of the baseline-LD model in each of 62 data sets analyzed. For each annotation, we report the enrichment of the annotation (i.e. proportion of heritability / proportion of SNPs, see[1]) and corresponding standard error. We also furnished enrichments when using the original baseline model from Finucane et al., and the baseline model used in this article (i.e. Finucane et al. baseline model + super/typical enhancer annotations + GERP annotations + 10 MAF bins). Results are meta-analyzed across 31 independent traits.

See Supplementary Excel file

Supplementary Table 9: Effect size and enrichment of each annotation of the baseline-LD model in each of 62 data sets analyzed. For each data set, we report the estimated effect sizes (both $\hat{\tau}$ and τ^*) and corresponding standard error and statistical significance, in addition of enrichments and corresponding standard error. For LD-related annotations, proportions of heritability are computed for the five quintiles of the annotation; first number is the proportion of heritability explained by the 20 % of the common SNPs with the lowest values of the annotation; last number is the proportion of heritability explained by the 20 % of the common SNPs with the highest values of the annotation. Predicted Allele Age* line gives the proportion of heritability explained after removing SNPs with missing ARGweaver allele age estimations.

	τ^* (se)	*P* value
LLD	-0.06 (0.03)	0.05
Predicted Allele Age	-0.25 (0.02)	1.60E-24
LLD-AFR	-0.16 (0.02)	5.16E-11
Recombination Rate (10 kb)	-0.2 (0.02)	2.69E-19
Nucleotide Diversity (10 kb)	-0.12 (0.02)	1.95E-11
Background Selection Statistic	0.12 (0.01)	4.39E-16
GC-Content (1,000 kb)	0.02 (0.02)	0.17
CpG-Content (50 kb)	0.22 (0.04)	5.46E-10

Supplementary Table 10: Effect size and statistical significance of the eight LD-related annotations fitted jointly with the baseline model and 10 MAF bins. We report the meta-analyzed effect size (τ^*) and corresponding standard error and statistical significance of eight LD-related annotations fitted jointly with baseline model and 10 MAF bins. These eight annotations are significant when fitted independently and conditioned on baseline model and MAF bins. Results are meta-analyzed across 31 independent traits. LLD and GC-content are no longer significant when fitted jointly with the baseline model and a total of eight LD-related annotations.

		Psychiatric diseases versus non-psychiatric diseases		Autoimmune diseases versus non- autoimmune diseases	
		τ^* (se)	*P* value	τ^* (se)	*P* value
Adjusted on 10 MAF bins	**Predicted Allele Age**	-0.83 (0.09) vs -0.76 (0.03)	0.46	-0.82 (0.10) vs -0.77 (0.03)	0.68
	LLD-AFR	-0.35 (0.03) vs -0.38 (0.02)	0.33	-0.46 (0.05) vs -0.38 (0.01)	0.11
	Recombination Rate (10 kb)	-0.92 (0.27) vs -0.53 (0.06)	0.16	-1.05 (0.23) vs -0.53 (0.06)	0.03
	Nucleotide Diversity (10 kb)	-0.66 (0.10) vs -0.8 (0.04)	0.18	-1.21 (0.08) vs -0.75 (0.04)	1.60E-07
	Background Selection Statistic	0.23 (0.10) vs 0.55 (0.05)	6.31E-03	1.46 (0.20) vs 0.47 (0.05)	1.02E-06
	CpG-Content (50 kb)	0.09 (0.10) vs 0.38 (0.04)	6.16E-03	0.75 (0.07) vs 0.32 (0.04)	1.78E-08
Adjusted on 10 MAF bins and baseline model	**Predicted Allele Age**	-0.61 (0.05) vs -0.44 (0.02)	1.24E-03	-0.43 (0.06) vs -0.46 (0.02)	0.69
	LLD-AFR	-0.23 (0.03) vs -0.15 (0.01)	0.01	-0.11 (0.04) vs -0.17 (0.02)	0.19
	Recombination Rate (10 kb)	-0.44 (0.11) vs -0.27 (0.03)	0.13	-0.53 (0.09) vs -0.27 (0.03)	3.57E-03
	Nucleotide Diversity (10 kb)	-0.31 (0.05) vs -0.26 (0.02)	0.40	-0.38 (0.05) vs -0.26 (0.02)	0.02
	Background Selection Statistic	0.09 (0.06) vs 0.12 (0.02)	0.66	0.20 (0.04) vs 0.11 (0.02)	0.07
	CpG-Content (50 kb)	0.21 (0.06) vs 0.15 (0.03)	0.37	-0.01 (0.07) vs 0.15 (0.03)	0.04

Supplementary Table 11: Effect size and statistical significance of the six LD-related annotations of the baseline-LD model in psychiatric and autoimmune diseases as compared to other traits. We report the meta-analyzed effect size (τ^*) and corresponding standard error and statistical significance of eight LD-related annotations fitted jointly with 10 MAF bins (first six lines) and fitted jointly with baseline model and 10 MAF bins (last six lines).
In first experiment, we observed significant larger effect of nucleotide diversity, the background selection statistics, and CpG-content in autoimmune diseases. In the second experiment, these effects are no longer significant, meaning that they were related to known functional annotations of the baseline model. MAF-adjusted predicted allele age become significant in the second experiment as effects were less heterogeneous between traits after conditioning on the baseline model (standard errors decreased from 0.09 to 0.05). The significance threshold was set to 0.05/24 = 2.08E-03.

	1st Quintile	2nd Quintile	3rd Quintile	4th Quintile	5th Quintile
Predicted Allele Age	31.12 (0.60)	25.45 (0.26)	15.46 (0.37)	19.08 (0.22)	8.90 (0.55)
Predicted Allele Age*	29.52 (0.59)	24.55 (0.22)	21.11 (0.06)	17.15 (0.24)	7.66 (0.54)
LLD-AFR	29.90 (0.35)	24.33 (0.15)	20.54 (0.09)	16.28 (0.17)	8.95 (0.32)
Recombination Rate (10 kb)	18.15 (0.46)	19.87 (0.21)	20.93 (0.17)	22.49 (0.20)	18.56 (0.56)
Nucleotide Diversity (10 kb)	28.92 (0.38)	24.19 (0.17)	20.74 (0.09)	17.11 (0.14)	9.04 (0.46)
Background Selection Statistic	13.02 (0.56)	16.88 (0.36)	19.97 (0.24)	23.02 (0.20)	27.11 (0.95)
CpG-Content (50 kb)	11.92 (0.70)	16.62 (0.54)	20.32 (0.22)	21.84 (0.39)	29.31 (1.03)
MAF	13.99 (0.47)	16.44 (0.52)	21.16 (0.59)	23.25 (0.81)	25.16 (0.67)

Supplementary Table 12: Percentage of heritability explained by five quintiles of each the six LD-related annotation of the baseline-LD model, meta-analyzed across 31 independent traits. We report results for each LD-related annotation of the baseline-LD model, and for MAF for comparison purposes. Predicted Allele Age* denotes the percentage of heritability explained after removing SNPs with missing ARGweaver allele age predictions. Numbers in parentheses are jackknife standard errors. 1st quintile represents the 20% of the common SNPs with the lowest values of the annotation; 5th quintile represents the 20% of the common SNPs with the highest values of the annotation.

		LLD-AFR			
		1st quintile	2nd-4th quintiles	5th quintile	
Recombination rate	1st quintile	2 % 2 % 1.08 (0.31)	9 % 12 % 1.35 (0.08)	9 % 4 % 0.48 (0.05)	20 % 18 % 0.92
	2nd-4th quintiles	10 % 22 % 2.35 (0.09)	40 % 37 % 0.91 (0.03)	10 % 5 % 0.51 (0.06)	60 % 64 % 1.07
	5th quintile	9 % 12 % 1.32 (0.12)	11 % 5 % 0.51 (0.06)	1 % 0 % 0.69 (0.21)	20 % 17 % 0.87
		20 % 36 % 1.79	60 % 54 % 0.90	20 % 10 % 0.50	

% of SNPs; % of h2g; enrichment (% of h2g / % of SNPs).

Supplementary Table 13: Opposing effects of recombination rate and LLD-AFR. We added to the baseline-LD model 9 binary annotations based on intersections of 3 recombination rate quintile bins and 3 LLD-AFR quintile bins (bins correspond to 1st quintile, 2nd to 4th quintiles, and 5th quintile). We report proportion of SNPs (in black), proportion of heritability (in blue), and enrichment (i.e. proportion of heritability divided by proportion of SNPs, in red; standard errors in parentheses) for each of these 9 annotations, as well as for the (non-intersected) 3 quintile bins of recombination rate and 3 quintile bins of LLD-AFR. We observed that the 3 quintile bins of recombination rate are not highly enriched or depleted for heritability (similar to Figure 4), but we observed strong effects of recombination rate (particularly for the largest recombination rate quintile) within the LLD-AFR bins. Results are meta-analyzed across 31 independent traits.

		CpG-Content 1st quintile	CpG-Content 2nd-4th quintiles	CpG-Content 5th quintile	
Recombination rate	1st quintile	6 % 4 % 0.60 (0.08)	11 % 11 % 0.99 (0.05)	3 % 5 % 1.80 (0.17)	20 % 20 % 0.98
	2nd-4th quintiles	12 % 8 % 0.64 (0.06)	37 % 36 % 0.98 (0.02)	11 % 19 % 1.74 (0.08)	60 % 63 % 1.06
	5th quintile	2 % 0 % 0.00 (0.13)	12 % 10 % 0.87 (0.07)	6 % 7 % 1.08 (0.09)	20 % 17 % 0.86
		20 % 11 % 0.57	60 % 58 % 0.96	20 % 31 % 1.54	

% of SNPs; % of h2g; enrichment (% of h2g / % of SNPs).

Supplementary Table 14: Opposing effects of recombination rate and CpG-Content. We added to the baseline-LD model 9 binary annotations based on intersections of 3 recombination rate quintile bins and 3 CpG-Content quintile bins (bins correspond to 1st quintile, 2nd to 4th quintiles, and 5th quintile). We report proportion of SNPs (in black), proportion of heritability (in blue), and enrichment (i.e. proportion of heritability divided by proportion of SNPs, in red; standard errors in parentheses) for each of these 9 annotations, as well as for the (non-intersected) 3 quintile bins of recombination rate and 3 quintile bins of CpG-Content. We observed that the 3 quintile bins of recombination rate are not highly enriched or depleted for heritability (similar Figure 4), but we observed strong effects of recombination rate (particularly for the largest recombination rate quintile) within the CpG-Content bins. Results are meta-analyzed across 31 independent traits.

	Standardized regression coefficient (x 10^{-5})
True Allele Age	-2.08 (0.08)
LLD-AFR	-1.50 (0.09)
Recombination Rate	-0.99 (0.10)
Nucleotide Diversity (10 kb)	-0.87 (0.08)

Supplementary Table 15: Forward simulations confirm that LD-related annotations predict deleterious effects. We report standardized regression coefficients for each of four LD-related annotations in a joint regression of absolute selection coefficient against these annotations and 10 MAF bins. These simulations were performed using an out-of-Africa demographic model and using d_1 = 0.60 and d_2 = 0.90 to model a non-homogeneous distribution of deleterious variants (see Online Methods). Numbers in parentheses are standard errors.

See Supplementary Excel file

Supplementary Table 16: Mean values of eight LD-related annotations in main functional annotations of the baseline model. We report means computed on common SNPs (MAF ≥ 5%).

		Mutation Rate				
		10 kb	**50 kb**	**100 kb**	**500 kb**	**1,000 kb**
CpG-Content	**10 kb**	0.88	.	.	.	.
	50 kb	.	0.86	.	.	.
	100 kb	.	.	0.85	.	.
	500 kb	.	.	.	0.86	.
	1,000 kb	.	.	.	.	0.87

Supplementary Table 17: Correlation between CpG-Content and local GoNL mutation rate map averaged across different genomic distances. We report correlations computed on common SNPs (MAF > 5%). Mutation rate of each reference SNPs have been computed by counting the number of A, C, G and T nucleotides and CpG dinucleotides in a surrounding window of the human reference sequence, and by using the 14 nucleotide/dinucleotide mutation rates estimated by GoNL[16] in 1 Mb windows (http://www.nlgenome.nl/?page_id=9). For regions of the genome with missing GoNL mutation rates, we used the mean nucleotide/dinucleotide mutation rates.

		Adjusted on MAF		Adjusted on MAF and baseline model	
		τ^* (se)	*P* value	τ^* (se)	*P* value
Mutation rate	**10 kb**	0.08 (0.03)	5.14E-03	-0.02 (0.02)	0.33
	50 kb	0.07 (0.03)	8.85E-03	-0.02 (0.02)	0.33
	100 kb	0.06 (0.03)	0.03	-0.03 (0.02)	0.21
	500 kb	0.03 (0.03)	0.32	-0.03 (0.02)	0.08
	1,000 kb	0.02 (0.02)	0.42	-0.03 (0.02)	0.11

Supplementary Table 18: Effect size and statistical significance of mutation rate annotations meta-analyzed across 31 independent traits. We report the meta-analyzed standardized effect size (τ^*) and corresponding standard error and statistical significance of the GoNL mutation rate annotations conditioned on 10 MAF bins (two first columns) and conditioned on the baseline model and 10 MAF bins (two last columns). See legend of Supplementary Table 16 for information about mutation rate annotations.

Model	Annotation	τ^*	P-value	Prop. SNPs	Prop. h_g^2	Enrichment
Baseline	Conserved	1.91 (0.28)	1.64E-11	2.57%	34.91%	13.59 (1.46)
Baseline + GERP NS	Conserved	1.53 (0.24)	2.97E-10	2.57%	30.89%	12.03 (1.25)
	GERP NS	0.73 (0.16)	2.73E-06	-	-	-
Baseline + GERP RS	Conserved	1.91 (0.29)	3.54E-11	2.57%	34.96%	13.61 (1.46)
	GERP RS	0.10 (0.24)	0.66	-	-	-
Baseline + GERP RS≥2	Conserved	1.46 (0.21)	1.08E-11	2.57%	32.18%	12.53 (1.27)
	GERP RS≥2	0.99 (0.21)	3.26E-06	6.39%	43.09%	6.74 (0.86)
Baseline + GERP RS≥3	Conserved	1.25 (0.21)	3.40E-09	2.57%	31.13%	12.12 (1.19)
	GERP RS≥3	1.08 (0.29)	1.95E-04	2.36%	26.88%	11.38 (1.78)
Baseline + GERP RS≥4	Conserved	1.24 (0.22)	3.33E-08	2.57%	30.80%	11.99 (1.22)
	GERP RS≥4	1.10 (0.27)	3.66E-05	0.81%	15.24%	18.70 (2.99)
Baseline + GERP NS + GERP RS≥2 + GERP RS≥3 + GERP RS≥4	Conserved	1.11 (0.20)	2.90E-08	2.57%	28.47%	11.08 (1.11)
	GERP NS	0.65 (0.15)	1.05E-05	-	-	-
	GERP RS≥2	0.05 (0.18)	0.77	6.39%	28.37%	4.44 (0.54)
	GERP RS≥3	0.16 (0.28)	0.56	2.36%	19.08%	8.08 (1.29)
	GERP RS≥4	0.60 (0.24)	1.38E-02	0.81%	12.13%	14.88 (2.32)
Baseline + GERP NS + GERP RS≥4	Conserved	1.11 (0.22)	5.29E-07	2.57%	28.49%	11.09 (1.15)
	GERP NS	0.67 (0.14)	3.66E-06	-	-	-
	GERP RS≥4	0.69 (0.19)	3.23E-04	0.81%	12.23%	15.00 (2.31)

Supplementary Table 19: Effect size and statistical significance of different GERP-related annotations. We report the standardized effect size (τ^*) and corresponding standard error and statistical significance, in addition of enrichments and corresponding standard error, for conserved annotations in different models. Different GERP related annotations were added to the baseline model in order to found the most informative ones. Here, the baseline model is composed of one binary annotation containing all SNPs, the 52 functional annotations of ref [1] that already contain a "Conserved" annotation from Lindblad-Toh et al.[17], four binary annotations based on super enhancers and typical enhancers[18], and 10 MAF bins. Results come from meta-analyses over the same nine independent traits than ref [1]. First, we observed that continuous annotation based on the neutral rate (NS) score was significant (P = 2.73E-06), while continuous annotation based on rejected substitutions (RS) score was not (P = 0.66). We thus created binary annotations using different threshold of RS score (2, 3 and 4). They were all significant when fitted independently, while only RS≥4 annotation is significant when all annotations are fitted jointly. We decided to update the baseline model with NS and RS≥4 annotations as they remain significant when they are fitted jointly, and as they bring information complementary to the Lindblad-Toh et al. "Conserved" annotation (which also remains significant). GERP NS and GERP RS continuous annotations have been MAF-adjusted.

	Reference panel	
	1000G Phase 3	**UK10K**
MAF bin 1	[5.01; 7.05]	[5.00; 7.08]
MAF bin 2	(7.05; 9.82]	(7.08; 9.78]
MAF bin 3	(9.82; 13.09]	(9.78; 13.05]
MAF bin 4	(13.09; 17.08]	(13.05; 16.95]
MAF bin 5	(17.08; 21.47]	(16.95; 21.39]
MAF bin 6	(21.47; 26.48]	(21.39; 26.37]
MAF bin 7	(26.48; 31.90]	(26.37; 31.85]
MAF bin 8	(31.90; 37.73]	(31.85; 37.66]
MAF bin 9	(37.73; 43.87]	(37.66; 43.76]
MAF bin 10	(43.87; 50.00]	(43.76; 50.00]

Supplementary Table 20: Boundaries of the 10 MAF bins used in stratified LD score regression analyses. We report boundaries of each MAF bin for both 1000G and UK10K reference panels.

Model	**Annotation**	τ^* **(se)**	***P* value**	**Proportion of heritability (se)**
MAF + Predicted Allele Age	Predicted Allele Age	-0.78 (0.03)	6.27E-175	-
MAF + Predicted Allele Age + Missing Allele Age	Predicted Allele Age	-0.81 (0.03)	2.09E-194	-
	Missing Allele Age	-0.47 (0.03)	6.67E-75	-0.044 (0.008)
Baseline + MAF + Predicted Allele Age	Predicted Allele Age	-0.46 (0.02)	2.38E-104	-
Baseline + MAF + Predicted Allele Age + Missing Allele Age	Predicted Allele Age	-0.47 (0.02)	1.65E-101	-
	Missing Allele Age	-0.14 (0.02)	5.40E-09	0.004 (0.005)

Supplementary Table 21: Effect size and statistical significance of predicted allele age with or without a binary annotation indicating common SNPs with missing ARGweaver allele age predictions. We report the standardized effect size (τ^*) and corresponding standard error and statistical significance, in addition of enrichments and corresponding standard error, for predicted allele age annotations in different models. Results are meta-analyzed across 31 independent traits.

See Supplementary Excel file

Supplementary Table 22: Information on LD-related annotations. We report means, standard deviations, medians, and top and bottom deciles and quartiles computed on common SNPs (MAF $\geq$ 5%).

	Null MAF-Independent Architecture	Null MAF-Dependent Architecture	Causal MAF+LD-Dependent Architecture
LLD	0.0008	-0.0096	-0.0067
Predicted Allele Age	-0.0011	-0.0085	-0.0112
LLD-AFR	0.0037	-0.0018	0.0015
Recombination Rate (10 kb)	-0.0249	-0.0248	-0.0275
Diversity (10 kb)	-0.0102	-0.0145	-0.0033
Background Selection Statistic	0.0061	0.0099	0.0194
CpG-Content (50 kb)	-0.0041	-0.0058	0.0015

Supplementary Table 23: Bias in estimates of standardized effect size τ^* for continuous LD-related annotations in simulations under three polygenic architectures. We report bias for each LD-related annotation in each simulation scenario.

	Null MAF-Independent Architecture	Null MAF-Dependent Architecture	Causal MAF+LD-Dependent Architecture
LLD	0.115 / 0.119	0.134 / 0.140	0.118 / 0.122
Predicted Allele Age	0.190 / 0.201	0.223 / 0.234	0.194 / 0.203
LLD-AFR	0.119 / 0.125	0.139 / 0.146	0.122 / 0.127
Recombination Rate (10 kb)	0.184 / 0.187	0.198 / 0.202	0.186 / 0.188
Diversity (10 kb)	0.085 / 0.089	0.096 / 0.101	0.088 / 0.093
Background Selection Statistic	0.064 / 0.068	0.072 / 0.078	0.080 / 0.085
CpG-Content (50 kb)	0.073 / 0.074	0.079 / 0.080	0.092 / 0.094

Supplementary Table 24: Calibration of standard errors in estimates of standardized effect size τ^* for continuous LD-related annotations in simulations under three polygenic architectures. We report the mean of the 10,000 standardized effect size τ^* standard error estimations (left number) and indicates the standard deviation of the 10,000 standardized effect size τ^* estimations (right number) for each LD-related annotation in each simulation scenario.

	Null MAF-Independent Architecture	Null MAF-Dependent Architecture	Causal MAF+LD-Dependent Architecture
LLD	0.0115	-0.0079	0.0585
Predicted Allele Age	-0.0001	-0.0079	0.0443
LLD-AFR	0.0126	-0.0010	0.0618
Recombination Rate (10 kb)	-0.0366	-0.0259	-0.0218
Diversity (10 kb)	-0.0087	-0.0123	0.0292
Background Selection Statistic	0.0039	0.0077	-0.0720
CpG-Content (50 kb)	-0.0062	-0.0060	-0.0837

Supplementary Table 25: Bias in estimates of standardized effect size τ^* for continuous LD-related annotations in simulations under three polygenic architectures with causal SNPs that are not in the reference panel. We report bias for each LD-related annotation in each simulation scenario.

Supplementary Figures

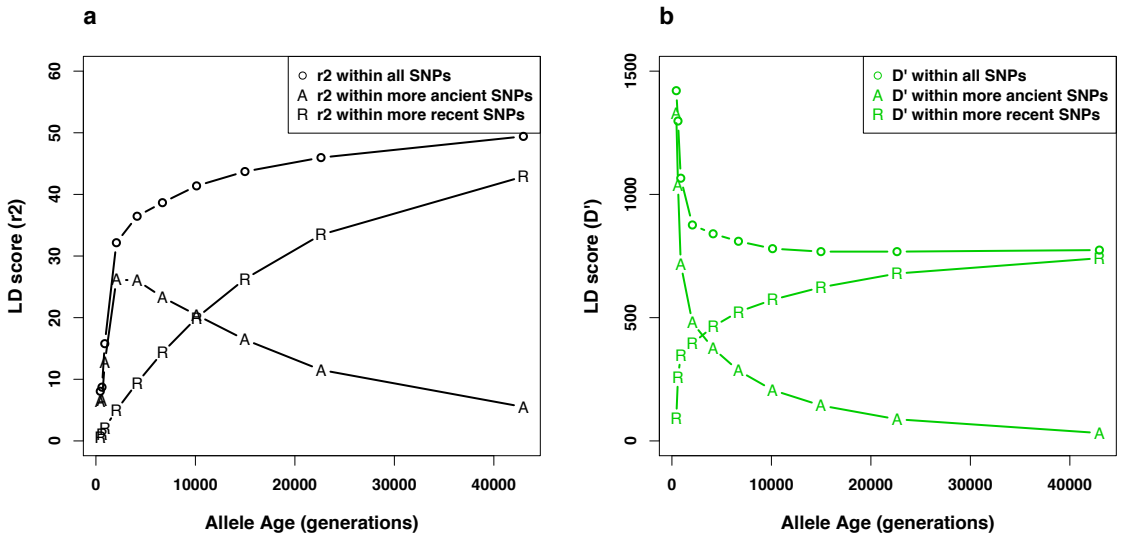

Supplementary Figure 1: Relationship between allele age and LD score. Coalescent simulations under Gravel et al. model[6] were performed to simulate a 33 Mb genome for 500 European individuals using ARGON software[5]. SNPs were grouped into 10 equal-sized bins based on allele age. LD scores of each SNP have been computed within a 1 cM window by summing r^2 coefficients (**a**), and by summing D' coefficients (**b**). For each SNP, these sums have been computed within all SNPs (open points), within its more ancient alleles (letters A) and within its more recent alleles (letters R). All SNPs with an allele count higher or equal to five have been considered (6,329,838 SNPs).

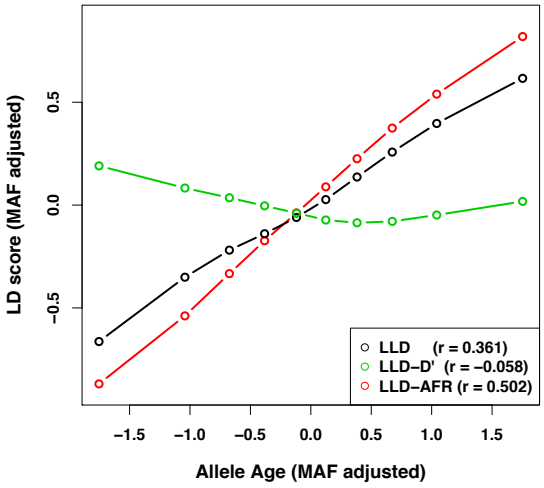

Supplementary Figure 2: Relationship between MAF-adjusted allele age and LLD. Coalescent simulations under Gravel et al. model[6] have been performed to simulate a 33 Mb genome for 500 European individuals and 500 African individuals using ARGON software[5]. Common SNPs (MAF $\geq$ 0.05, 3,823,497 SNPs) were grouped into 10 equal-sized bins based on MAF-stratified allele age.

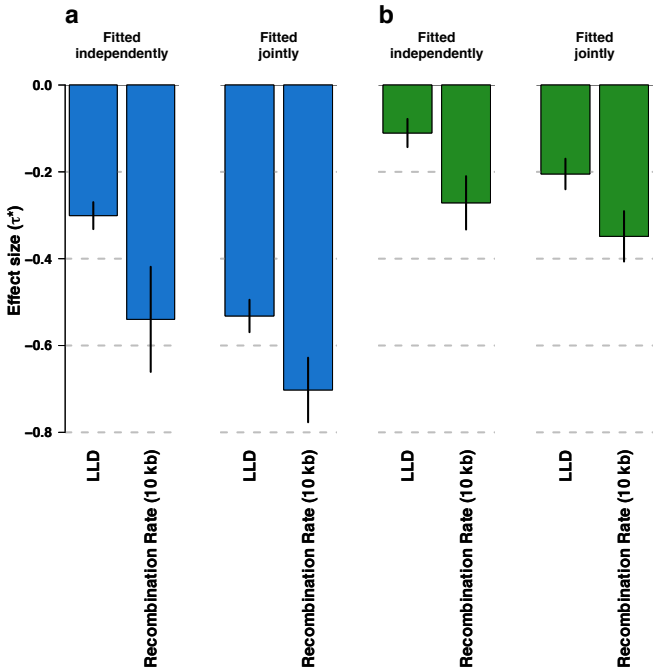

Supplementary Figure 3: Opposing effects of LLD and recombination rate annotations. (a) Meta-analysis results for LLD and recombination rate annotations, conditioned on 10 MAF bins. **(b)** Meta-analysis results for LLD and recombination rate annotations, conditioned on 10 MAF bins and on baseline model. Results are meta-analyzed across 31 independent traits.

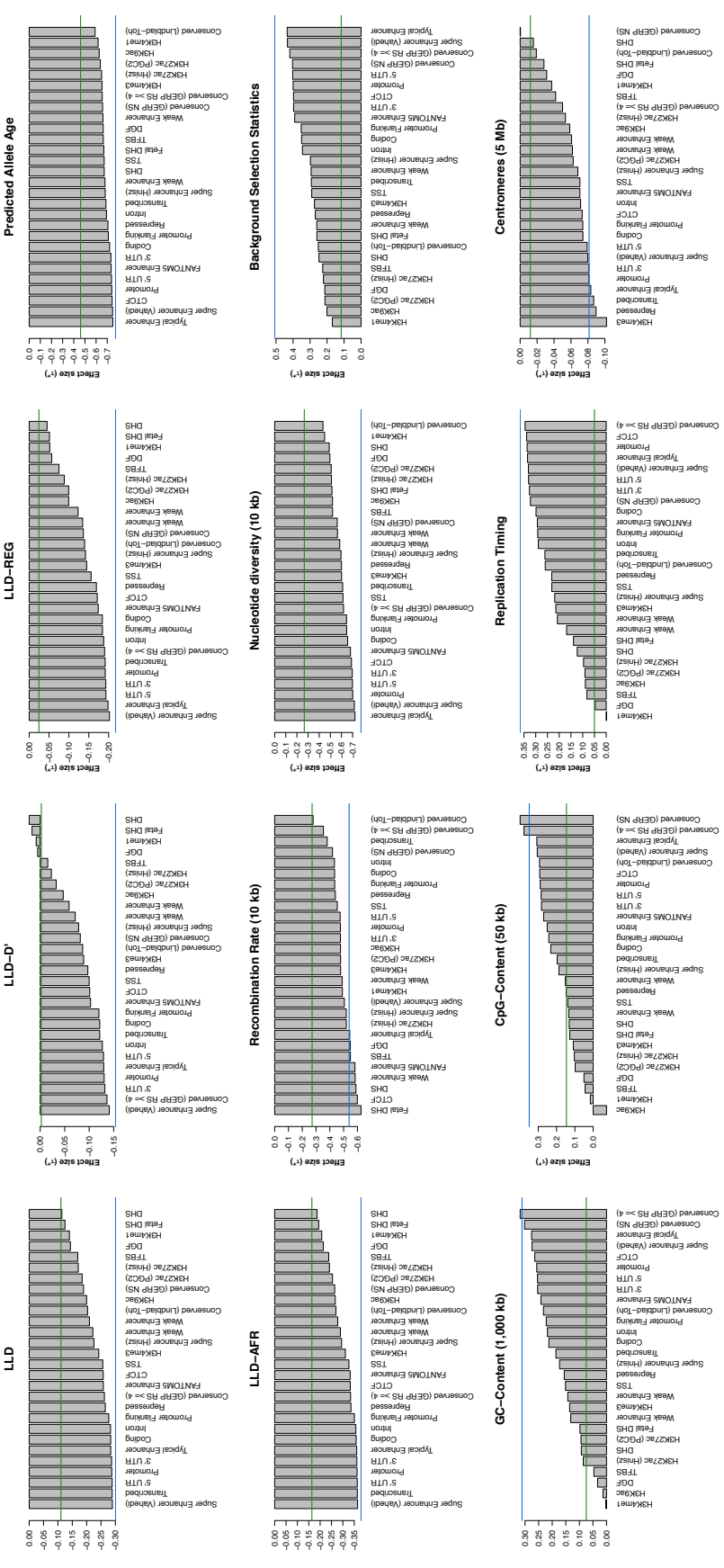

Supplementary Figure 4: Effect sizes of 12 LD-related annotations conditioned on one main functional annotation from the baseline model at a time. Each bar represents the per-standardized effect size of one LD-related annotation conditioned on 10 MAF bins and one functional annotation. The blue line is the effect size of the LD-related annotation conditioned on 10 MAF bins; the green line is the effect size of the LD-related annotation conditioned on 10 MAF bins and the baseline model. Results are meta-analyzed across 31 independent traits. We note that inclusion of the DHS annotation removes as much LLD signal as the entire baseline model.

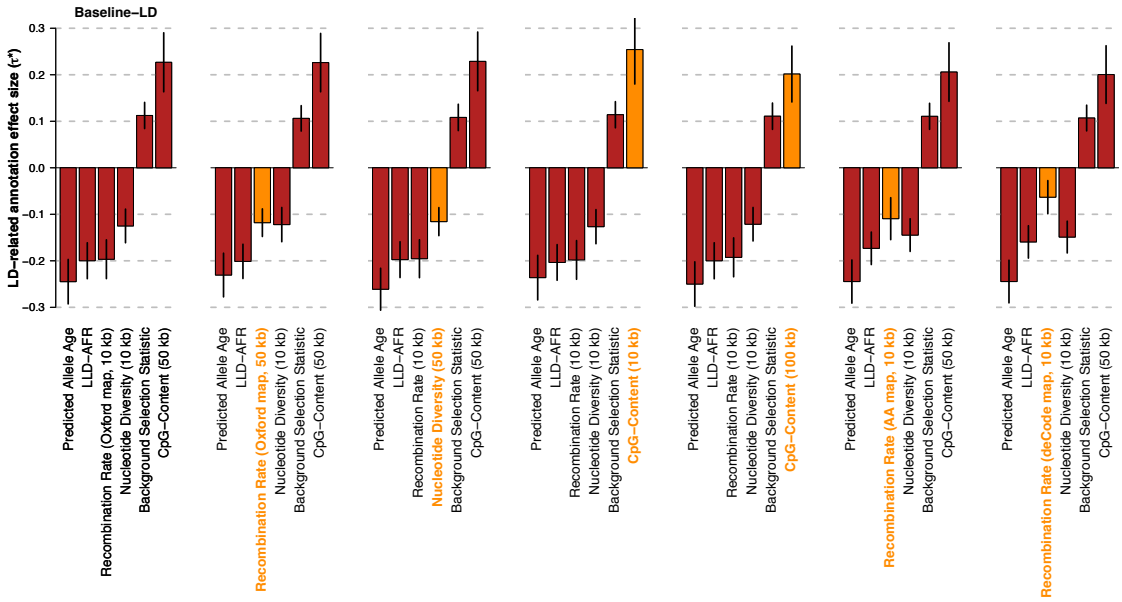

Supplementary Figure 5: Effect sizes of LD-related annotations when changing (one at a time) the window size for a window-based annotation or the data source for recombination rate in the baseline-LD model. We report the standardized effect size (tau*) and corresponding jackknife 95% confidence intervals for each LD-related annotation of the baseline-LD models. The modified annotation is indicated in orange. Results are meta-analyzed across 31 independent traits.

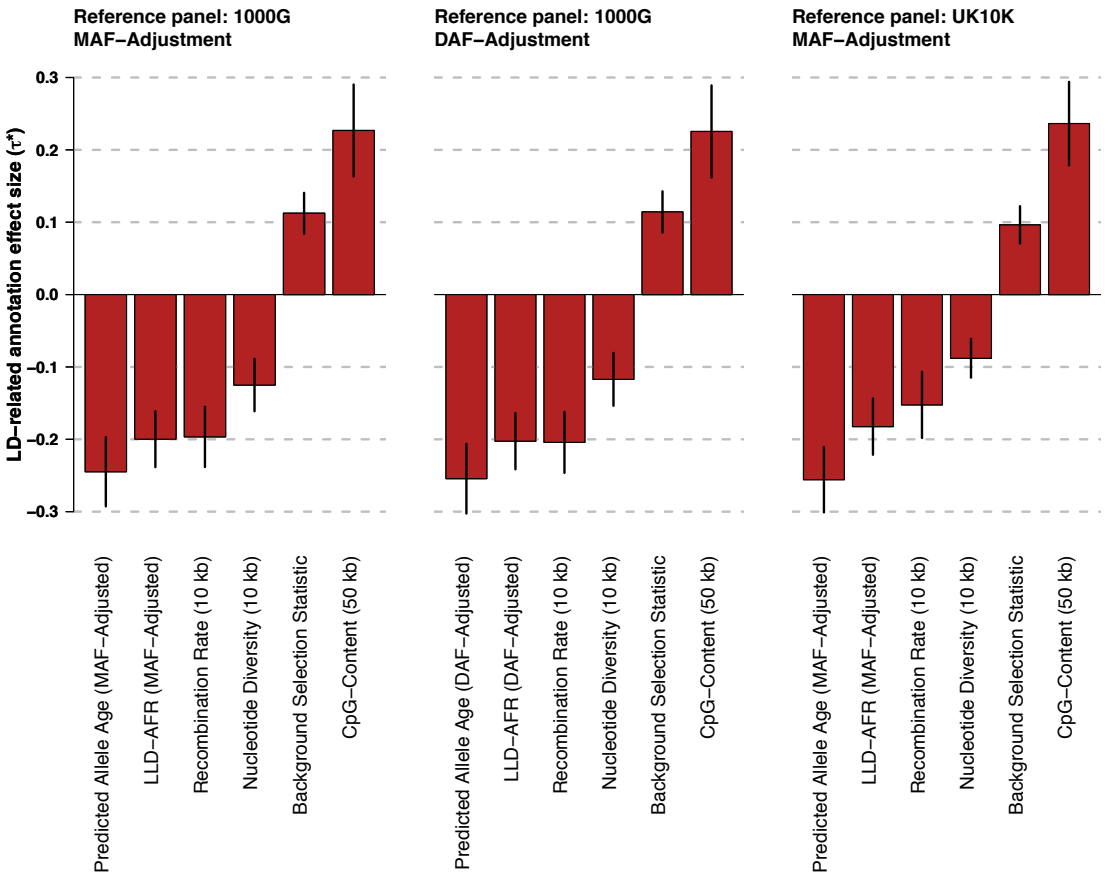

Supplementary Figure 6 Results of the baseline-LD model using DAF-adjustment andUK10K reference panel. The left graph represents joint effects of the 6 LD-related annotations in the baseline-LD model, using 489 European of 1000 Genomes (1000G) project as a reference panel for stratified LD score and MAF-adjustment (graph similar than Figure 3a). The middle graph uses 10 DAF bins (instead of 10 MAF bins), and predicted allele age and LLD-AFR are DAF-adjusted (instead of MAF-adjusted). The right graph uses 3,567 individuals of UK10K database as a reference panel (instead of 1000G).

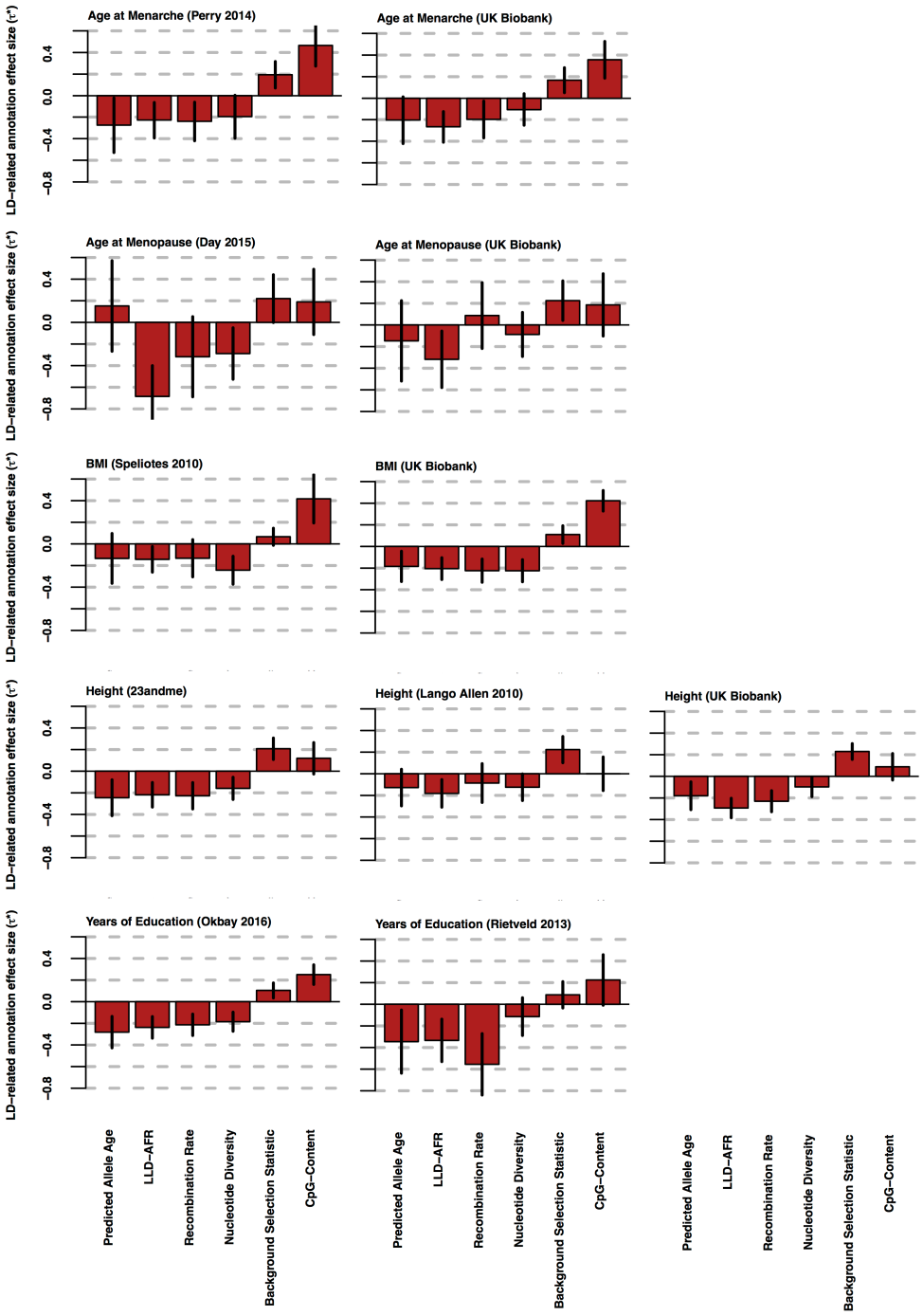

Supplementary Figure 7: Results of the baseline-LD model across different data sets for the same trait. We report the standardized effect size (τ^*) and corresponding jackknife 95% confidence intervals for each LD-related annotation of the baseline-LD model. We observed no significantly different effects for annotations of the same trait. Numerical results are reported in Supplementary Table 9.

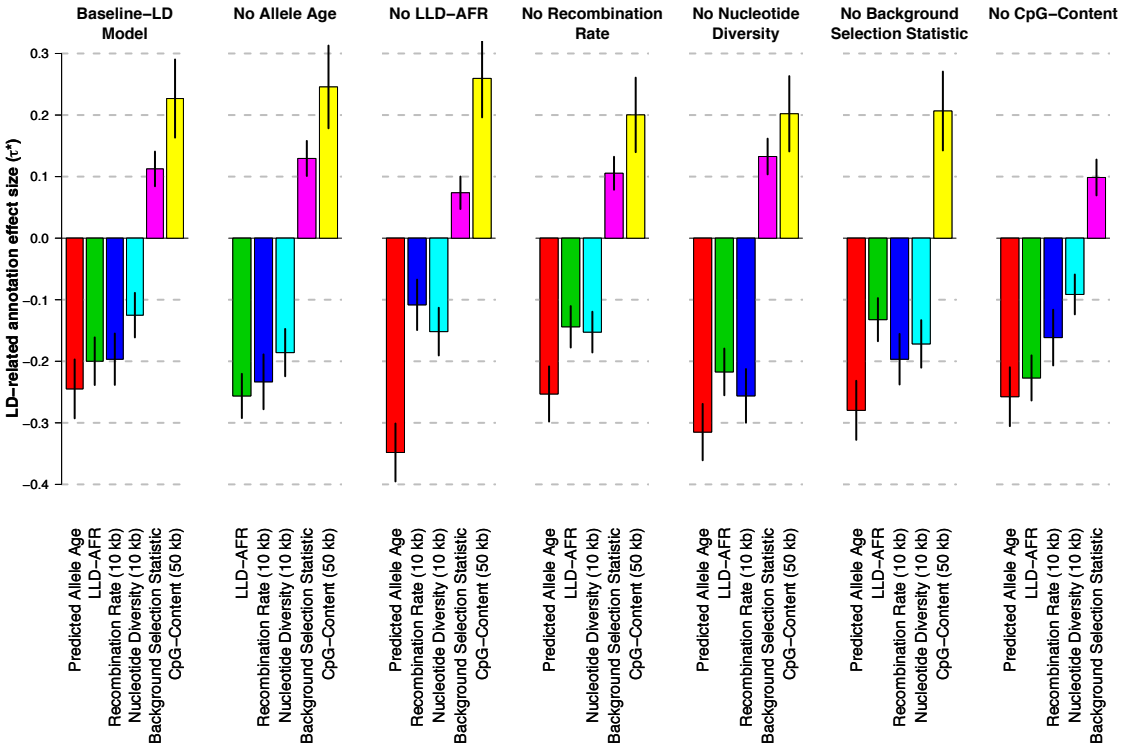

Supplementary Figure 8: Effect sizes of LD-related annotations when removing one LD-related annotation at a time from the baseline-LD model. We report the standardized effect size (τ^*) and corresponding jackknife 95% confidence intervals for each LD-related annotation of the baseline-LD models. Results are meta-analyzed across 31 independent traits.

See pdf file Figure_S09.pdf.

Supplementary Figure 9: Proportion of heritability explained by the quintiles of each LD-related annotation of the baseline-LD model, for each of the 62 data sets analyzed. We report results for each LD-related annotation of the baseline-LD model, and for MAF for comparison purposes.

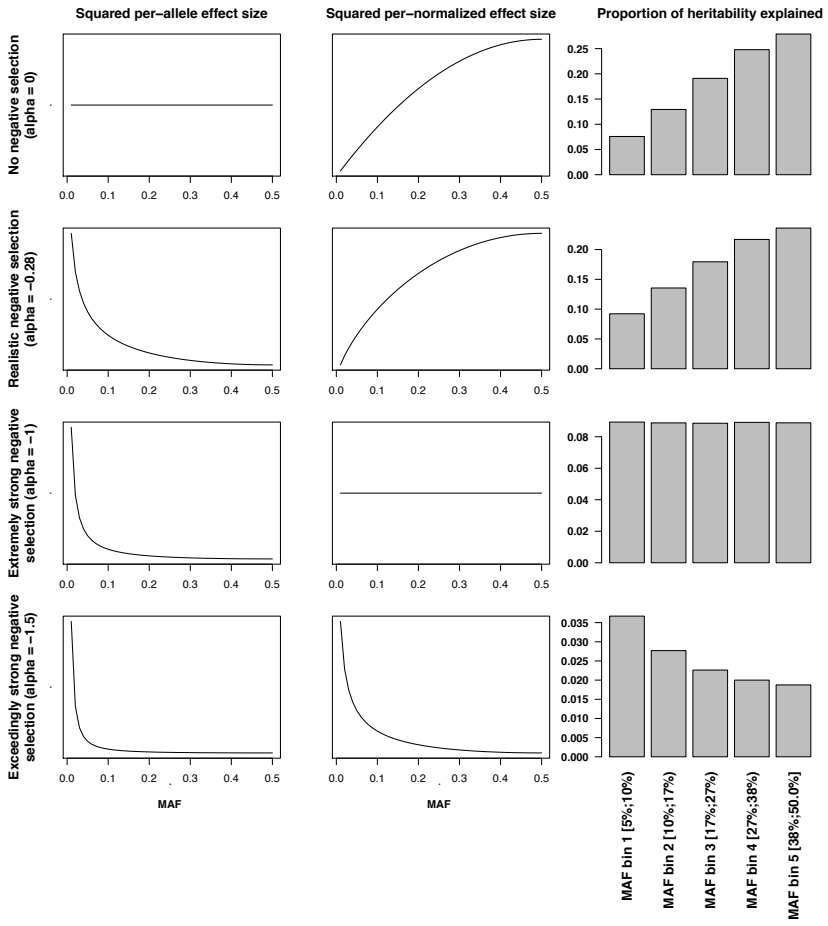

Supplementary Figure 10: Relationship between negative selection and MAF-dependent architecture. Under a genetic model where per-allele effect size has mean 0 and variance proportional to $\big(p(1-p)\big)^{\alpha}$, we report the mean squared per-allele effect size (proportional to $\big(p(1-p)\big)^{\alpha}$), the mean squared per-normalized genotype effect size (proportional to $\big(p(1-p)\big)^{\alpha+1}$), and the corresponding proportion of heritability explained by quintile MAF bins with equal numbers of common SNPs (proportional to per-SNP heritability). These values were computed from chromosome 1 SNPs with MAF $\geq$ 0.1% in UK10K. Quintile MAF bins were restricted to common SNPs, analogous to Figure 4. We considered four different model of negative selection: *i*) no negative selection (α = 0); *ii*) realistic negative selection (α = -0.28, as previously estimated for schizophrenia[19]); *iii*) extremely strong negative selection (α = -1); *iv*) exceedingly strong negative selection (α = -1.5). This figure demonstrates that slightly smaller per-SNP heritability for less common variants is expected under realistic levels of negative selection. We note that a separate question that we do not consider in detail is what happens when SNPs are grouped into equally spaced MAF bins (note that less common equally spaced MAF bins will contain more SNPs than more common equally spaced MAF bins). Previous work has shown that, under negative selection, less common equally spaced MAF bins (with more SNPs) will explain more variance than more common equally spaced MAF bins (with fewer SNPs); see Figure 4a of ref. [20].

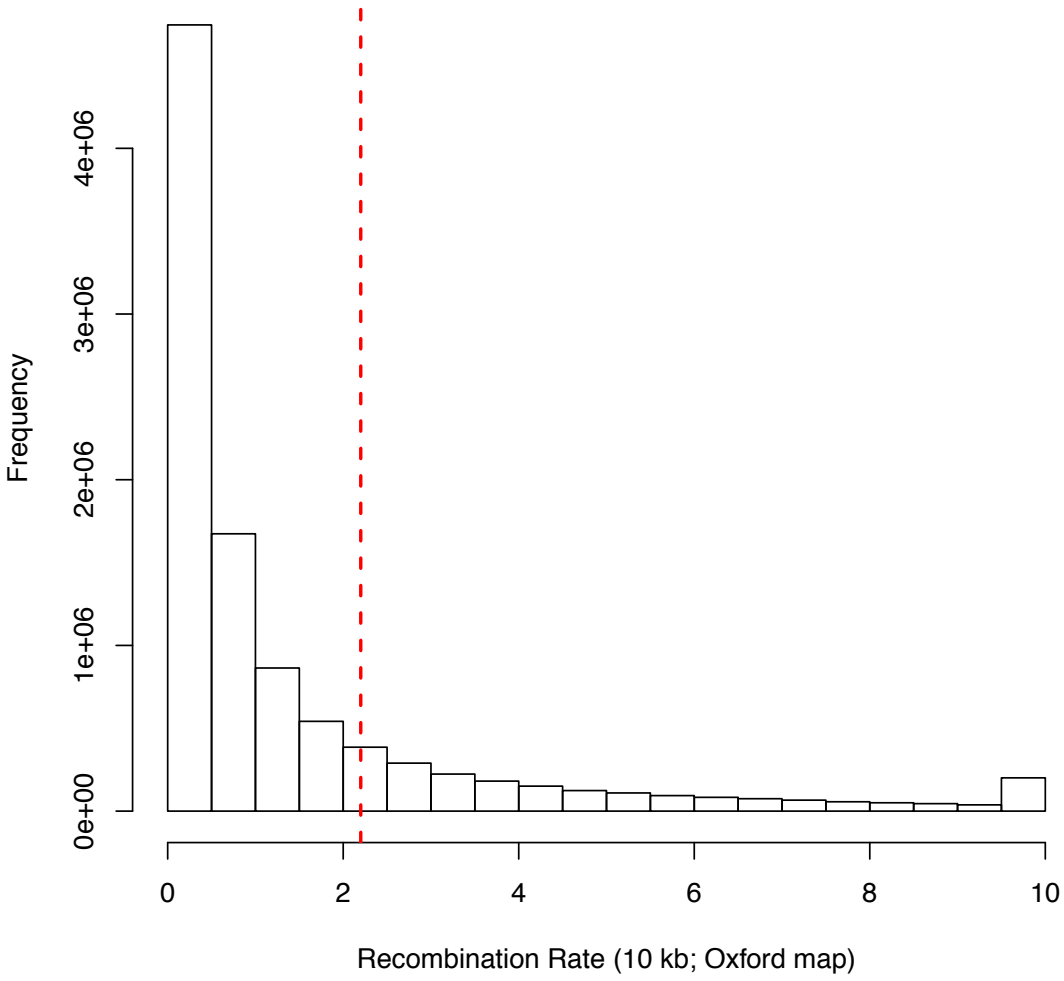

Supplementary Figure 11: Distribution of the recombination rate annotation. Values are capped at 10 cM/Mb for illustrative purposes. The dashed red line indicates the start of the 5th quintile of recombination rate displayed in Figure 4.

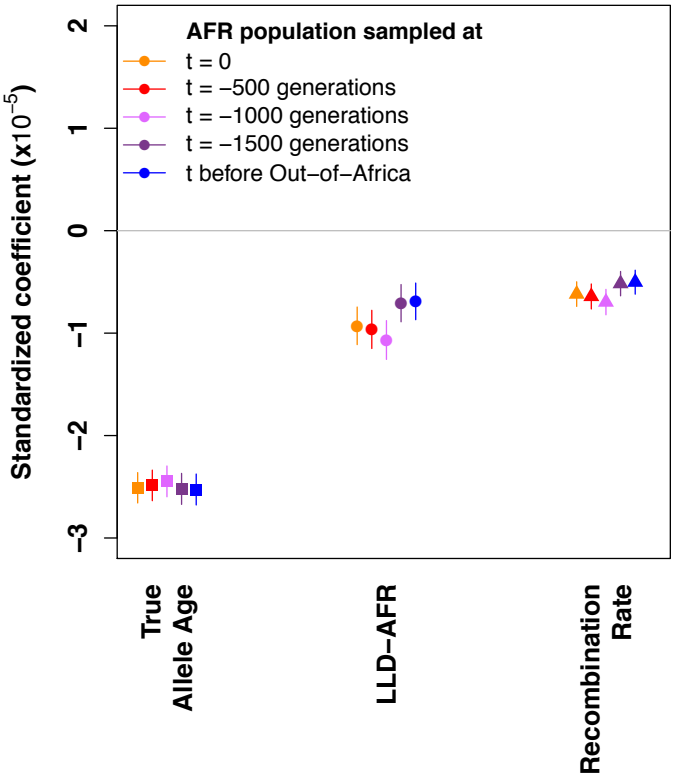

Supplementary Figure 12: Results of forward simulations when sampling the AFR population at different generations in the past. We performed forward simulations[21] using a demographic out-of-Africa model for populations of African and European descent[6] and assessed their link with the absolute value of the selection coefficient $|s|$. We chose a homogeneous distribution of deleterious variants (d = 0.75) to remove confounding of nucleotide diversity annotation. We report the standardized regression coefficients for the three LD-related annotations in a joint regression of absolute selection coefficient against these annotations and 10 MAF bins. Error bars represent 95% confidence intervals around the regression coefficient estimates.

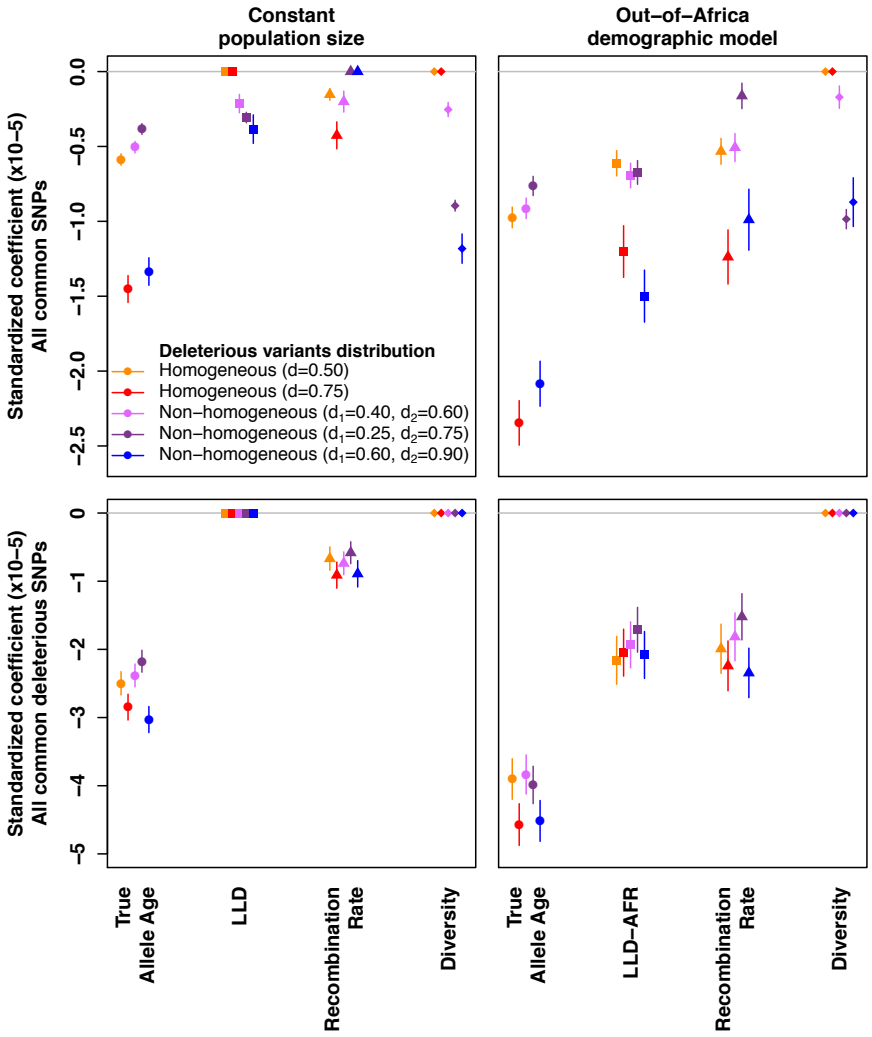

Supplementary Figure 13: Results of forward simulations under different demographic models and deleterious variants distributions. We performed forward simulations[21] using two demographic models: a constant population size of 10,000 individuals (first column) and the out-of-Africa model for populations of African and European descent[6] (second column). Deleterious SNPs (i.e. $s \neq 0$) were distributed homogeneously with proportion d, or non-homogeneously by altering proportions d_1 and d_2. Simulations integrated coldspots and high recombination rate regions[22]. We report the standardized regression coefficients for the four LD-related annotations in a joint regression of absolute selection coefficient against these annotations and 10 MAF bins. LLD was considered instead of LLD-AFR in the constant population size demographic model. A linear regression was performed over all common SNPs to find which annotations allow distinguishing deleterious variants to neutral ones (first line), and over all common deleterious SNPs to find which annotations drive the magnitude of the selection coefficient s (second line). Standardized regression coefficient of 0 indicates that the annotation was not significant and was removed to re-compute the coefficients of the remaining annotations. Error bars represent 95% confidence intervals around the regression coefficient estimates.

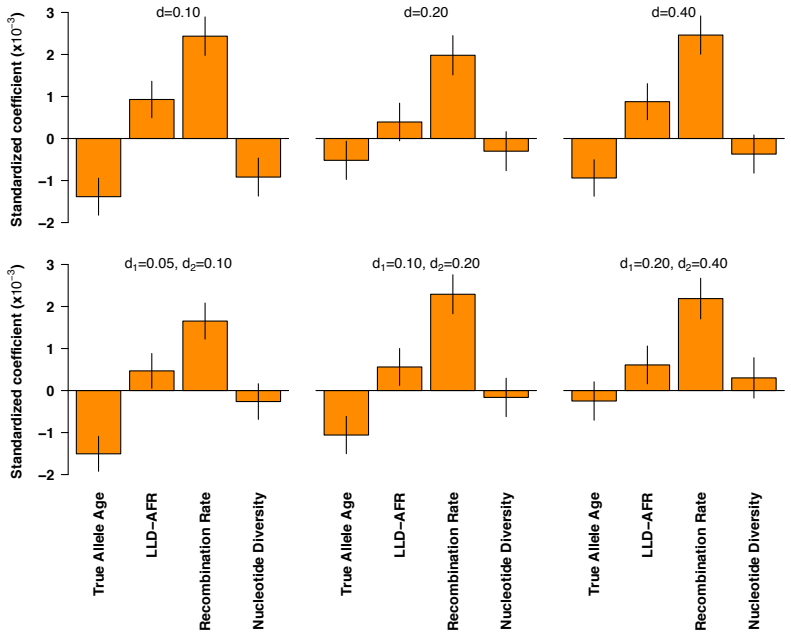

Supplementary Figure 14: Forward simulations confirm that LD-related annotations do not predict beneficial effects. We performed forward simulations[7] using a demographic out-of-Africa model for populations of African and European descent[5]. Beneficial SNPs were distributed homogeneously with proportion d (first panel), or non-homogeneously by altering proportions d_1 and d_2 (second panel) using proportions similar to those in Enard et al.[23]. Selection coefficients s were drawn from an exponential distribution with mean 0.01. We report standardized regression coefficients for each of four LD-related annotations in a joint regression of absolute selection coefficient against these annotations in data from forward simulations. Error bars represent 95% confidence intervals around the regression coefficient estimates. We observed that results for LLD-AFR and recombination rate do not correspond to the standardized effect sizes for trait heritability reported in Figure 3c.

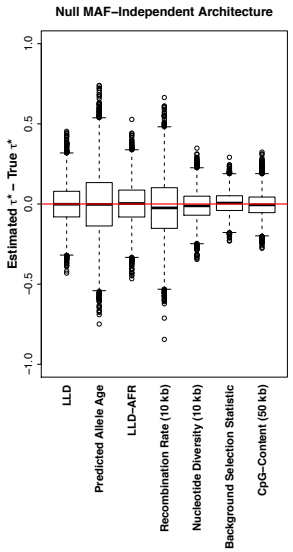

Supplementary Figure 15: Bias in estimates of standardized effect size τ^* for continuous LD-related annotations in simulations under a null MAF-independent architecture. We report bias (estimated vs. true τ^*) across 10,000 simulations for null simulations with MAF-independent architecture.

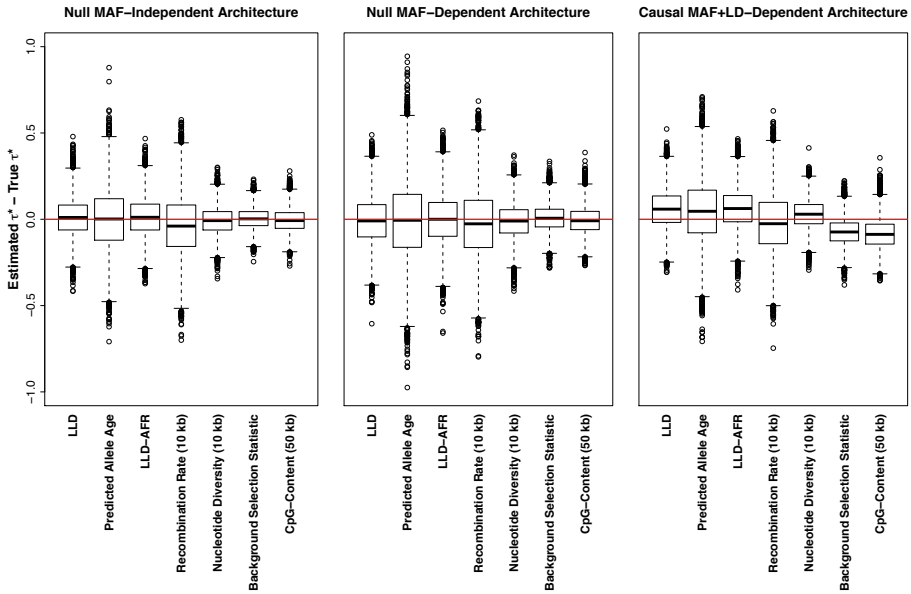

Supplementary Figure 16: Bias in estimates of standardized effect size τ^* for continuous LD-related annotations in simulations under 3 polygenic architectures with causal SNPs that are not in the reference panel. We report bias (estimated vs. true τ^*) across 10,000 simulations for null simulations with MAF-independent architecture (left), null simulations with MAF-dependent architecture (center) and causal simulations with MAF+LD-dependent architecture (right).

References

1. Finucane, H. K. *et al.* Partitioning heritability by functional annotation using genome-wide association summary statistics. *Nat. Genet.* **47,** 1228–1235 (2015).
2. Gazal, S., Sahbatou, M., Babron, M.-C., Génin, E. & Leutenegger, A.-L. High level of inbreeding in final phase of 1000 Genomes Project. *Sci. Rep.* **5,** 17453 (2015).
3. The 1000 Genomes Project Consortium. A global reference for human genetic variation. *Nature* **526,** 68–74 (2015).
4. The UK10K Consortium. The UK10K project identifies rare variants in health and disease. *Nature* **526,** 82–90 (2015).
5. Palamara, P. F. ARGON: fast, whole-genome simulation of the discrete time Wright-fisher process. *Bioinforma. Oxf. Engl.* (2016). doi:10.1093/bioinformatics/btw355
6. Gravel, S. *et al.* Demographic history and rare allele sharing among human populations. *Proc. Natl. Acad. Sci.* **108,** 11983–11988 (2011).
7. Palamara, P. F. *et al.* Leveraging Distant Relatedness to Quantify Human Mutation and Gene-Conversion Rates. *Am. J. Hum. Genet.* **97,** 775–789 (2015).
8. Eriksson, N. *et al.* Web-Based, Participant-Driven Studies Yield Novel Genetic Associations for Common Traits. *PLOS Genet* **6,** e1000993 (2010).
9. Tung, J. Y. *et al.* Efficient Replication of over 180 Genetic Associations with Self-Reported Medical Data. *PLOS ONE* **6,** e23473 (2011).
10. Durand, E. Y., Do, C. B., Mountain, J. L. & Macpherson, J. M. Ancestry Composition: A Novel, Efficient Pipeline for Ancestry Deconvolution. *bioRxiv* 010512 (2014). doi:10.1101/010512
11. Henn, B. M. *et al.* Cryptic Distant Relatives Are Common in Both Isolated and Cosmopolitan Genetic Samples. *PLOS ONE* **7,** e34267 (2012).
12. 1000 Genomes Project Consortium. A map of human genome variation from population-scale sequencing. *Nature* **467,** 1061–1073 (2010).
13. Browning, S. R. & Browning, B. L. Rapid and accurate haplotype phasing and missing-data inference for whole-genome association studies by use of localized haplotype clustering. *Am. J. Hum. Genet.* **81,** 1084–1097 (2007).
14. Fuchsberger, C., Abecasis, G. R. & Hinds, D. A. minimac2: faster genotype imputation. *Bioinformatics* **31,** 782–784 (2015).
15. Loh, P.-R. *et al.* Efficient Bayesian mixed-model analysis increases association power in large cohorts. *Nat. Genet.* **47,** 284–290 (2015).
16. Francioli, L. C. *et al.* Genome-wide patterns and properties of de novo mutations in humans. *Nat. Genet.* **47,** 822–826 (2015).
17. Lindblad-Toh, K. *et al.* A high-resolution map of human evolutionary constraint using 29 mammals. *Nature* **478,** 476–482 (2011).
18. Vahedi, G. *et al.* Super-enhancers delineate disease-associated regulatory nodes in T

cells. *Nature* **520,** 558–562 (2015).

19. Loh, P.-R. *et al.* Contrasting genetic architectures of schizophrenia and other complex diseases using fast variance-components analysis. *Nat. Genet.* **47,** 1385–1392 (2015).

20. Yang, J. *et al.* Genetic variance estimation with imputed variants finds negligible missing heritability for human height and body mass index. *Nat. Genet.* **47,** 1114–1120 (2015).

21. Messer, P. W. SLiM: Simulating Evolution with Selection and Linkage. *Genetics* **194,** 1037–1039 (2013).

22. Hussin, J. G. *et al.* Recombination affects accumulation of damaging and disease-associated mutations in human populations. *Nat. Genet.* **47,** 400–404 (2015).

23. Enard, D., Messer, P. W. & Petrov, D. A. Genome-wide signals of positive selection in human evolution. *Genome Res.* (2014). doi:10.1101/gr.164822.113